Check for updates

Kinetics-controlled regulation for homogeneous nucleation and growth of colloidal polymer and carbon nanospheres†

Quan-Gao Wang, Lu Hou and An-Hui Lu [iD] *

Size regulation of uniform polymer nanospheres (PNSs) and carbon nanospheres (CNSs) below 100 nm has been difficult and is limited by multiple factors, such as ongoing nucleation, Ostwald ripening, minimization of surface energy, and high viscosity during the nucleation and growth process. In this study, a kinetics-controlled regulation is reported for the synthesis of monodispersed PNSs and corresponding CNSs with adjustable size below 100 nm. During the synthesis of PNSs, three distinct stages including surface energy control, surface tension control and viscosity control have been observed, where the concentration of block copolymer F127 (C_{F127}) plays a vital role in affecting the nucleation rate of PNSs and tunes the diffusion rate of monomers and migration of particles during the nucleation and growth process. As a consequence, the size of monodisperse CNSs can be customized from 100 nm down to 41 nm with PDI below 5%.

Polymeric and carbonaceous nanospheres have potential applications in water purification,[1,2] drug delivery,[3,4] photonic inks,[5,6] environmental sensors,[7,8] and energy storage and conversion.[9,10] The success of these applications is highly determined by the availability of nanospheres with controllable composition, tunable size and monodispersity, especially when the particle dispersion index (PDI) of nanospheres is below 5%.

Although various synthetic strategies have been developed for the preparation of monodisperse PNSs and corresponding CNSs, the size regulation of spheres in the nanoscale has been limited by some barriers. For example, (1) the ongoing nucleation prevents all of the nuclei from emerging at the same time and growing at the same growth rate with the over-supply of the monomer, which ultimately leads to broad size distribution.[11] (2) Ostwald ripening is an unavoidable process which manifests itself as the growth of large particles at the expense of smaller ones and broadens the standard deviation of the particle size distribution.[12,13] (3) In general, surface energy increases as the particle size decreases, *e.g.*, the surface energy of 4 nm nanoparticles increase over 45% compared to that of 40 nm nanoparticles with identical structure.[14,15] Hence, the smaller nanoparticles tend to minimize the total surface energy by reconstructing the surface morphology and structure,[16] thus forming aggregated large particles. (4) The high viscosity of the polymerization reaction system restricts the diffusion of monomers and brings about polydisperse particles.[17] Apparently, simultaneously controlling so many growth factors of one-pot synthesis is indeed difficult when considering the sphere's uniformity and size at the nanometer level.

To address these abovementioned issues, we hereby report a facile and operable kinetics-controlled regulation for the synthesis of polymer nanospheres (PNSs) and corresponding carbon nanospheres (CNSs) with good monodispersity and precisely tailorable size. The kinetics control is realized by adjusting the surface tension and viscosity *via* the use of an appropriate concentration of block copolymer F127 (C_{F127}), so that the size of PNSs and the corresponding CNSs can be customized below 100 nm with excellent uniformity. To our knowledge, it is rather rare to find such a report on the preparation of CNSs with customizable and uniform size from 100 nm down to 41 nm, with polydispersity index less than 5%. Our study would provide a material platform for fundamental structure–performance investigations on electrochemistry, catalyst, adsorption, *etc.*

In the homogeneous nucleation process of polybenzoxazines nanospheres, the energy barrier and nucleation rate of the homogeneous nucleation are interpreted thermodynamically (see S3, ESI†). Based on the analysis of the nucleation kinetics, the surface tension is one of the critical factors in adjusting the nucleation rate according to eqn (9) (see Fig. S3, ESI†), which further plays a crucial role in the regulation of particle size and morphology.[18–20] To control the nucleation kinetics of PNSs, a detailed study was conducted through adjusting the surface tension during the nucleation process *via* changing the concentration of block copolymer F127 (C_{F127}).

State Key Laboratory of Fine Chemicals, School of Chemical Engineering, Dalian University of Technology, Dalian 116024, P. R. China. E-mail: anhuilu@dlut.edu.cn
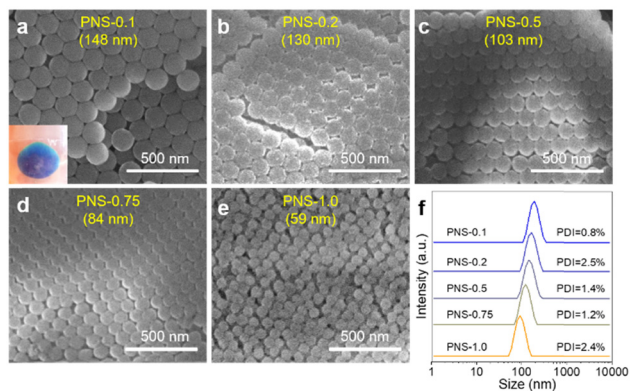
Fig. 1 (a–e) SEM images and (f) particle size distribution curves of the PNSs-0.1, PNSs-0.2, PNSs-0.5, PNSs-0.75, and PNSs-1.0. The inset in panel (a) is the photograph of PNSs-0.1 after centrifugation.

Fig. 2 The evolution of solution viscosity of (a) PNSs-0.1 and (b) PNSs-1.5. (c) Schematic representation of nucleation and growth of monodisperse PNSs *via* the kinetics-controlled regulation method.

Upon mixing ethylamine with a resorcinol/formaldehyde/F127 solution, a white solution was obtained in several minutes. Firstly, when the initial C_{F127} was 0.1 g L^{-1}, the final size of the obtained monodisperse PNSs (denoted PNSs-0.1) was 148 nm (Fig. 1a). A self-assembled periodic structure with close-packed planes arranged along the (111) direction was observed, indicating an excellent monodispersity of the obtained PNSs-0.1.[21,22] Dynamic light scattering (DLS) results demonstrated that the particle dispersion index (PDI) of the PNSs-0.1 was only 0.8% (Fig. 1f), indicating the good monodispersity of the PNSs-0.1. The uniformity of PNSs-0.1 can also be further confirmed by the bright blue structural color of PNSs-0.1 after centrifugal separation (Fig. 1a, inset). This was attributed to the self-assembly of PNSs-0.1 into colloidal crystals *via* high-speed centrifugation,[23] again strong evidence of high uniformity of the PNSs. There is no obvious structural color for other PNSs due to their smaller sizes, as shown in Fig. S1 (ESI†).

It was generally accepted that the surface tension decreased during the modulating process of increasing the C_{F127} when the C_{F127} was less than the critical micelle concentration (CMC_{F127}, here the CMC_{F127} was 2.5 g L^{-1} when the temperature is 28 °C). When the initial C_{F127} was 0.1 g L^{-1}, the surface tension of the solution is only 41.2 mN m^{-1} (Fig. S2, ESI†). By gradually controlling the C_{F127} in the order of 0.2, 0.5, 0.75, and 1.0 g L^{-1}, the surface tension of the solution gradually decreased from 41.2 to 37.6 mN m^{-1}. The synthesized PNSs, which were denoted as PNSs-0.2, PNSs-0.5, PNSs-0.75, and PNSs-1.0, can be finely adjusted to 130, 103, 84, and 59 nm (Fig. 1b–e). Notably, all PDIs of the PNSs were below 5% (Fig. 1f) when the C_{F127} was between 0.1–1.0 g L^{-1}, which was essential in the construction of three-dimensional periodic structures by self-assembly.[24] The monodispersity information from DLS analysis was also in accordance with SEM observations (Fig. 1). Obviously, the lower the surface tension, the smaller the size of the PNSs is. It also can be explained by the homogeneous nucleation and growth theory. Lower surface tension can facilitate nucleation to form more nuclei, which consequently leads to smaller PNSs. At this point, surface tension is one of the key parameters that can adjust the nucleation kinetics of the PNSs. This may pave another simple
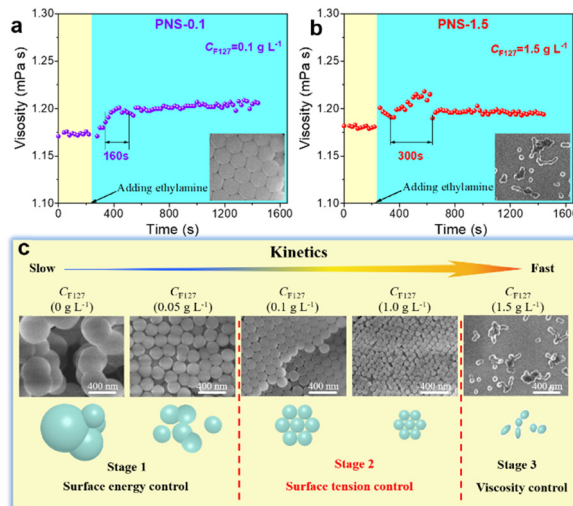
and convenient way for the customization of PNSs with nanoscale size *via* such a kinetics-controlled process by adjusting the surface tension.

When excessive F127 (*e.g.* 1.5 g L^{-1}) was used in the synthesis, the size of the PNSs-1.5 decreased to 52 nm with the further decrease of the surface tension. Unexpectedly, the PNSs-1.5 showed irregular morphology and became polydisperse (Fig. S3a, ESI†), and the PDI of PNSs-1.5 also increased to 6.7% (Fig. S3e, ESI†). In order to clarify the reason for the polydispersity of PNSs, the viscosity of the reaction system was investigated during the nucleation and growth process, as shown in Fig. 2a and b. Before the addition of ethylamine, the viscosity of the resorcinol/formaldehyde/F127 solution slightly increased as the initial C_{F127} increased. The variation of viscosity probably was caused by the changing hydrogen bonds during the nucleation and growth process. It is worthwhile mentioning that the more hydrogen bonds are formed, the larger the viscosity is.[24] Before the addition of ethylamine, the viscosity was determined by the hydrogen bonding among water, resorcinol, formaldehyde, and the PEO blocks of F127. Therefore, the PNSs-0.1 possessed lower viscosity (1.17 mPa s^{-1}, Fig. 2a) than the PNSs-1.5 (1.18 mPa s^{-1}, Fig. 2b) due to the decreased number of hydrogen bonds by reducing the C_{F127} before the nucleation process. Upon the addition of ethylamine, the reaction process involves a rapid increase in the concentration of monomers (oligomer) until a critical concentration is achieved, and fast consumption of free monomers (and oligomers) due to the nucleation growth, which has been described by the homogeneous nucleation and growth theory. After the addition of ethylamine, the viscosity of PNSs-0.1 increased from 1.17 mPa s^{-1} to 1.20 mPa s^{-1} and decreased around 1.19 mPa s^{-1} in 160 s, as reflected by a small peak.[25] And the PNSs-0.1 possessed uniform morphology and monodisperse size (PDI = 0.8%) (Fig. 1a and f). However, when excessive F127 was added to the system (*e.g.* 1.5 g L^{-1}), the viscosity of PNSs-1.5

sharply increased from 1.18 mPa s^{-1} to 1.22 mPa s^{-1}, but gradually decreased to 1.19 mPa s^{-1} over 300 s, as reflected by a broad peak. Finally, the PNSs-1.5 showed irregular morphology and a polydisperse particle size distribution (PDI = 6.7%, Fig. S3e, ESI†). The difference in the evolution of viscosity was mainly caused by the number of hydrogen bonds between monomers (oligomers) and hydrophilic PEO blocks of F127[26,27] with changing the C_{F127}. The higher C_{F127}, the higher the viscosity during the nucleation and growth process was. The higher viscosity limited the diffusion of monomers and the migration of particles, which may result in continuous nucleation and different growth probability of particles. Thus, the PNSs exhibited irregular morphology and broad size distribution.[28] The lower viscosity can facilitate the diffusion of monomers and the short variation time of the viscosity exhibits fast consumption of free monomers, which was in favor of separating the primary nucleation and subsequent growth process and thus guaranteed the good uniformity of the nanospheres.

When the C_{F127} was further increased over the CMC_{F127} (e.g. 3.0 g L^{-1}), PNSs-3.0 possessed a hollow structure (Fig. S3b, ESI†) and the PDI of the PNSs-3.0 was 15.4% (Fig. S3f, ESI†), which was due to the aggregation of hollow polymer particles. Conversely, when an insufficient amount of F127 was used in the synthesis (e.g. 0.05 g L^{-1}, γ = 42.5 mN m^{-1}, Fig. S2, ESI†), the slow nucleation rate brought about the large sized PNSs-0.05, which possessed an average size of 201 nm. Interestingly, a small fraction of dimers can be found from the SEM image (Fig. S3c, ESI†) and the PDI of PNSs-0.05 was 8.1% (Fig. S3g, ESI†). The dimers indicated that the primary polymeric particles were prone to merging with each other or fusing together into large particles, thus reducing the surface energy with the insufficiency of F127. In the absence of F127, the solution showed a higher surface tension (γ = 64.0 mN m^{-1}, Fig. S2, ESI†) resulting in a slower nucleation rate and consequently larger size of PNSs-0. The SEM images of PNSs-0 showed that some irregular aggregates were formed (Fig. S3d, ESI†). And macrophase red sediment was produced after the reaction (Fig. S3h, ESI†). The big aggregated particles indicated that the aggregation of primary particles and continuous nucleation took place in the whole process without F127. The spontaneous aggregation of primary polymeric particles was driven by the minimum surface energy when using an insufficient amount of F127, in this case, the C_{F127} was below 0.1 g L^{-1}.

Based on the above observation and analysis, we can conclude that PNSs with uniform size can be customized in the nanoscale by the kinetics-controlled synthesis, where the C_{F127} has a vital role in reducing the surface energy and adjusting the surface tension and viscosity of the synthetic system. The C_{F127} would affect the nucleation rate of PNSs and tune the diffusion rate of monomers and migration of particles during the nucleation and growth process. Fig. 2c schematically illustrates three distinct stages observed for the nucleation and growth of PNSs with different C_{F127}.

When there is no surfactant F127 or an insufficient amount of F127 (C_{F127} was below 0.1 g L^{-1}, Stage 1) in the reaction system, the size regulation of PNSs is under surface energy control (Fig. 3a). The higher surface tension (over 41.2 mN m^{-1},
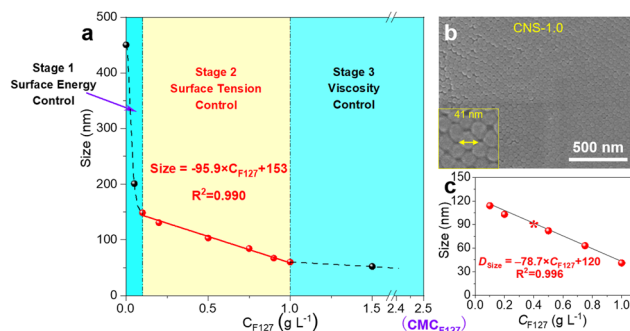

Fig. 3 (a) The relationship between the size of PNSs and the concentration of F127. (b) SEM image of the representative sample CNSs-1.0, and (c) the correlation between the C_{F127} and the size of CNSs.

Fig. S2, ESI†) of the reaction system leads to the lower nucleation rate of PNSs, and thus less nuclei and consumption of monomers. Moreover, due to the insufficiency of F127 to stabilize the primary polymeric particles, the primary polymeric particles aggregate to reduce the surface energy. As a result, the surplus monomers are enough for a continual cascading of nuclei. Eventually, large nanoparticles and some aggregated dimers are formed (Fig. S3c and d, ESI†).

Upon increasing the C_{F127} to a feasible concentration range (0.1–1.0 g L^{-1}, Stage 2), the precise size regulation of PNSs is realised under the synergetic function of surface energy and viscosity (Fig. 3a). We defined this stage as the surface tension control stage to differ it from the surface energy stage. With increasing C_{F127}, the surface tension can be precisely adjusted from 41.2 to 37.6 mN m^{-1} (Fig. S2, ESI†), so that the corresponding nucleation rate increases (see eqn (5), Fig. S3, ESI†). It should be pointed out that the faster nucleation rate leads to faster consumption of free monomers and more polymeric nuclei. The size of the resultant monodispersed PNSs decreased with the decreasing of the surface tension gradually (Fig. 1a–e). Self-assembled periodic structures are observed in the SEM images of all the as-prepared PNSs, indicating the excellent monodispersity of all PNSs. The uniform morphology is also confirmed by DLS analysis (Fig. 1f) together with the photonic crystal phenomenon after high-speed centrifugation. The average size of the PNSs increased during the whole nucleation and growth process in Stage 2 (Fig. S4a, ESI†), while the PDI of the PNSs remained below 5% (Fig. S4b, ESI†), which indicated that all the polymer particles undergo the same nucleation and growth period, which is of great importance for the uniformity control. The size and monodispersity regulation of PNSs in Stage 2 is ascribed to the faster nucleation rate and lower viscosity. The faster nucleation is beneficial to separate the primary nucleation process and subsequent growth; meanwhile, the lower viscosity promotes the diffusion of the monomer and migration of particles, ensuring good monodispersity of PNSs. The regulation of C_{F127} allows facile control over the surface tension during the nucleation process, which is significant for the customization of monodisperse PNSs at the nanoscale.

With a high initial C_{F127} (1.0 g L^{-1}-CMC_{F127}, Stage 3), the size and morphology regulation of the PNSs is under viscosity

control (Fig. 3a). In this case, when the surface tension decreases further (below 37.6 mN m^{-1}), the size of PNSs-1.5 further decreases to ~52 nm (Fig. S3a, ESI†). However, the morphology of the PNSs becomes polydisperse and irregular, and the PDI of PNSs-1.5 is up to 6.7% (Fig. S3e, ESI†). The investigation of viscosity elucidates that the diffusion of monomers and the migration of particles are limited by the higher viscosity in the nucleation and growth process. This led to continuous nucleation and different growth probability of the particles, leading to the broad size distribution and polydispersity of the PNSs.

There is a linear relationship between C_{F127} and the size of PNSs in Stage 2. A good linear function was obtained (Fig. 3a) by using the C_{F127} (0.1–1.0 g L^{-1}) and the size of the PNSs with linear fitting. These results clearly demonstrate that F127 molecules play a critical role in the customization of PNSs with nanoscale size and excellent monodispersity. The F127 molecules can stabilize the primary polymeric particles to reduce the surface energy during the nucleation process. The proper C_{F127} can adjust the surface tension to facilitate the diffusion rate of monomers, which can ultimately affect the nucleation rate, size and monodispersity of PNSs at the nanoscale.

Followed by the pyrolysis of PNSs in Stage 2 at 500 °C, the obtained CNSs well inherited the uniform morphology, size, and periodic structures of PNSs (Fig. S5, ESI† and Fig. 3b). The average sizes of CNSs-0.1, CNSs-0.2, CNSs-0.5, CNSs-0.75, and CNSs-1.0 were 114, 103, 82, 63, and 41 nm, respectively. A good linear correlation between C_{F127} and the size of the CNSs was obtained (Fig. 3c), of which the correlation coefficient was 0.996. In order to verify the accuracy of this linear relationship, an additional experiment was carried out. For example, when the C_{F127} was set as 0.4 g L^{-1}, the actual size of the CNSs-0.4 was 92 nm (Fig. S6a and b, ESI†), while the calculated size of the CNSs was 88 nm. Hence, the size of the CNSs can be precisely adjusted at the nanoscale by varying the C_{F127}, ensuring a good uniformity. The N$_2$ adsorption–desorption isotherms of CNSs-0.4 showed a typical type I curve (Fig. S6c, ESI†), indicating that CNSs-0.4 possessed a microporous feature. The sharp nitrogen uptake at the relative pressure range of 0.9–1.0 was attributed to nitrogen molecule condensation in the nanospaces among the close-packed CNSs. The Brunauer–Emmett–Teller surface area of CNSs-0.4 was 587 m^2 g^{-1}. The pore size distribution of CNSs-0.4 showed a narrow peak at 0.55 nm (Fig. S6d, ESI†), implying the microporous feature.

In summary, we have demonstrated a facile and operable kinetics-controlled method for the regulation of PNSs and corresponding CNSs with excellent monodispersity at the nanoscale through precisely controlling the appropriate surface tension by changing the C_{F127}.

Conflicts of interest

There are no conflicts to declare.

Notes and references

1 Y. H. Xue, W. Teng, Y. Y. Chen, Q. Ma, X. Q. Chen, Y. Sun, J. W. Fan, Y. P. Qiu and R. B. Fu, *Chem. Eng. J.*, 2022, **429**, 132262.
2 J. M. Zhao, R. Luque, W. J. Qi, J. P. Lai, W. Y. Gao, M. R. Gilani and G. B. Xu, *J. Mater. Chem. A*, 2015, **3**, 519–524.
3 L. M. Wang, Q. Sun, X. Wang, T. Wen, J. J. Yin, P. Y. Wang, R. Bai, X. Q. Zhang, L. H. Zhang, A. H. Lu and C. Y. Chen, *J. Am. Chem. Soc.*, 2015, **137**, 1947.
4 P. F. Gao, L. L. Zheng, L. J. Liang, X. Y. Yang, Y. F. Li and C. Z. Huang, *J. Mater. Chem. B*, 2013, **1**, 3202.
5 S. H. Kim, V. Hwang, S. G. Lee, J. W. Ha, V. N. Manoharan and G. R. Yi, *Small*, 2019, **15**, 1900931.
6 Y. W. Song, K. J. Fang, M. N. Bukhari, K. Zhang and Z. Y. Tang, *J. Mol. Lig.*, 2021, **324**, 114702.
7 L. K. Gil-Herrera, J. A. Pariente, F. Gallego-Gómez, F. Gándara, B. H. Juárez, A. Blanco and C. López, *Adv. Funct. Mater.*, 2017, 1703885.
8 J. T. Zhang, L. L. Wang, D. N. Lamont, S. S. Velankar and S. A. Asher, *Angew. Chem.*, 2012, **124**, 6221.
9 S. Chen, L. L. Zhao, J. Z. Ma, J. Q. Wang, L. M. Dai and J. T. Zhang, *Nano Energy*, 2019, **60**, 536.
10 T. Liu, L. Y. Zhang, B. Cheng and J. G. Yu, *Adv. Energy Mater.*, 2019, **9**, 1803900.
11 Y. Wang, J. He, C. Cui, W. H. Chong and H. Chen, *Angew. Chem., Int. Ed.*, 2015, **54**, 2022.
12 B. Liu and H. C. Zeng, *Small*, 2005, **1**, 566.
13 J. Park, J. Joo, S. G. Kwon, Y. J. Jang and T. Hyeon, *Angew. Chem., Int. Ed.*, 2007, **46**, 4630.
14 H. M. Lu and Q. Jiang, *J. Phys. Chem. B*, 2004, **108**, 5617.
15 G. Ouyang, C. X. Wang and G. W. Yang, *Chem. Rev.*, 2009, **109**, 4221.
16 L. H. Zhang, B. He, W. C. Li and A. H. Lu, *Adv. Energy Mater.*, 2017, 1701511.
17 K. Pancholi, N. Ahras, E. Stride and M. Edirisinghe, *J. Mater. Sci.: Mater. Med.*, 2009, **20**, 917.
18 W. Li, J. Yang, Z. Wu, J. Wang, B. Li, S. Feng, Y. Deng, F. Zhang and D. Y. Zhao, *J. Am. Chem. Soc.*, 2012, **134**, 11864.
19 Q. Yue, J. L. Li, Y. Zhang, X. W. Cheng, X. Chen, P. P. Pan, J. C. Su, A. A. Elzatahry, A. Alghamdi, Y. H. Deng and D. Y. Zhao, *J. Am. Chem. Soc.*, 2017, **139**, 4954.
20 X. G. Wang, Q. Cheng, Y. Yu and X. Z. Zhang, *Angew. Chem., Int. Ed.*, 2018, **57**, 7836.
21 M. Agrawal, D. Fischer, S. Gupta, N. E. Zafeiropoulos, A. Pich, E. Lidorikis and M. Stamm, *J. Phys. Chem. C*, 2010, **114**, 16389.
22 J. H. Zhang, Y. E. Li, X. M. Zhang and B. Yang, *Adv. Mater.*, 2010, **22**, 4249.
23 C. X. Hua, H. B. Xu, P. P. Zhang, X. Y. Chen, Y. Y. Lu, Y. Gan, J. P. Zhao and Y. Li, *Colloid Polym. Sci.*, 2017, **295**, 1655.
24 Y. Ma, Y. Liu, H. S. Su, L. Wang and J. L. Zhang, *J. Mol. Liq.*, 2018, **255**, 176.
25 T. Ngo and H. Yang, *J. Phys. Chem. Lett.*, 2015, **6**, 5051.
26 C. D. Liang and S. Dai, *J. Am. Chem. Soc.*, 2006, **128**, 5316.
27 J. Tang, J. Liu, C. Li, Y. Li, M. Tade, S. Dai and Y. Yamauchi, *Angew. Chem., Int. Ed.*, 2015, **54**, 588.
28 H. Y. Zhao, F. Zhang, S. M. Zhang, S. He, F. Shen, X. G. Han, Y. D. Yin and C. B. Gao, *Nano Res.*, 2018, **11**, 3814.